

NASA-TM-83593

DOE/NASA/51040-52
NASA TM-83593

NASA-TM-83593

19840018416

Real-Time Simulation of an Automotive Gas Turbine Using the Hybrid Computer

FOR REFERENCE

NOT TO BE TAKEN FROM THIS ROOM

William Costakis and Walter C. Merrill
National Aeronautics and Space Administration
Lewis Research Center

LIBRARY COPY

May 1984

5/14/84 1984

LANGLEY RESEARCH CENTER
LIBRARY, NASA
HAMPTON, VIRGINIA

Prepared for
U.S. DEPARTMENT OF ENERGY
Conservation and Renewable Energy
Office of Vehicle and Engine R&D

DISCLAIMER

This report was prepared as an account of work sponsored by an agency of the United States Government. Neither the United States Government nor any agency thereof, nor any of their employees, makes any warranty, express or implied, or assumes any legal liability or responsibility for the accuracy, completeness, or usefulness of any information, apparatus, product, or process disclosed, or represents that its use would not infringe privately owned rights. Reference herein to any specific commercial product, process, or service by trade name, trademark, manufacturer, or otherwise, does not necessarily constitute or imply its endorsement, recommendation, or favoring by the United States Government or any agency thereof. The views and opinions of authors expressed herein do not necessarily state or reflect those of the United States Government or any agency thereof.

Printed in the United States of America

Available from

National Technical Information Service
U.S. Department of Commerce
5285 Port Royal Road
Springfield, VA 22161

NTIS price codes¹

Printed copy: A02

Microfiche copy: A01

¹Codes are used for pricing all publications. The code is determined by the number of pages in the publication. Information pertaining to the pricing codes can be found in the current issues of the following publications, which are generally available in most libraries: *Energy Research Abstracts (ERA)*; *Government Reports Announcements and Index (GRA and I)*; *Scientific and Technical Abstract Reports (STAR)*; and publication, NTIS-PR-360 available from NTIS at the above address.

7 1 1 RN/NASA-TM-83593
DISPLAY 07/2/1
84N26484** ISSUE 16 PAGE 2569 CATEGORY 85 RPT#: NASA-TM-83593
E-1994 DOE/NASA/51040-52 NAS(1.15)83593 CNT#: DE-AI01-77CS-51040
84/05/00 26 PAGES UNCLASSIFIED DOCUMENT

UTL: Real-time simulation of an automotive gas turbine using the hybrid computer TLSP: Final Report

AUTH: A/COSTAKIS, W.; B/MERRILL, W. C.

CORP: National Aeronautics and Space Administration, Lewis Research Center, Cleveland, Ohio. AVAIL. NTIS SAP: HC A03/MF A01

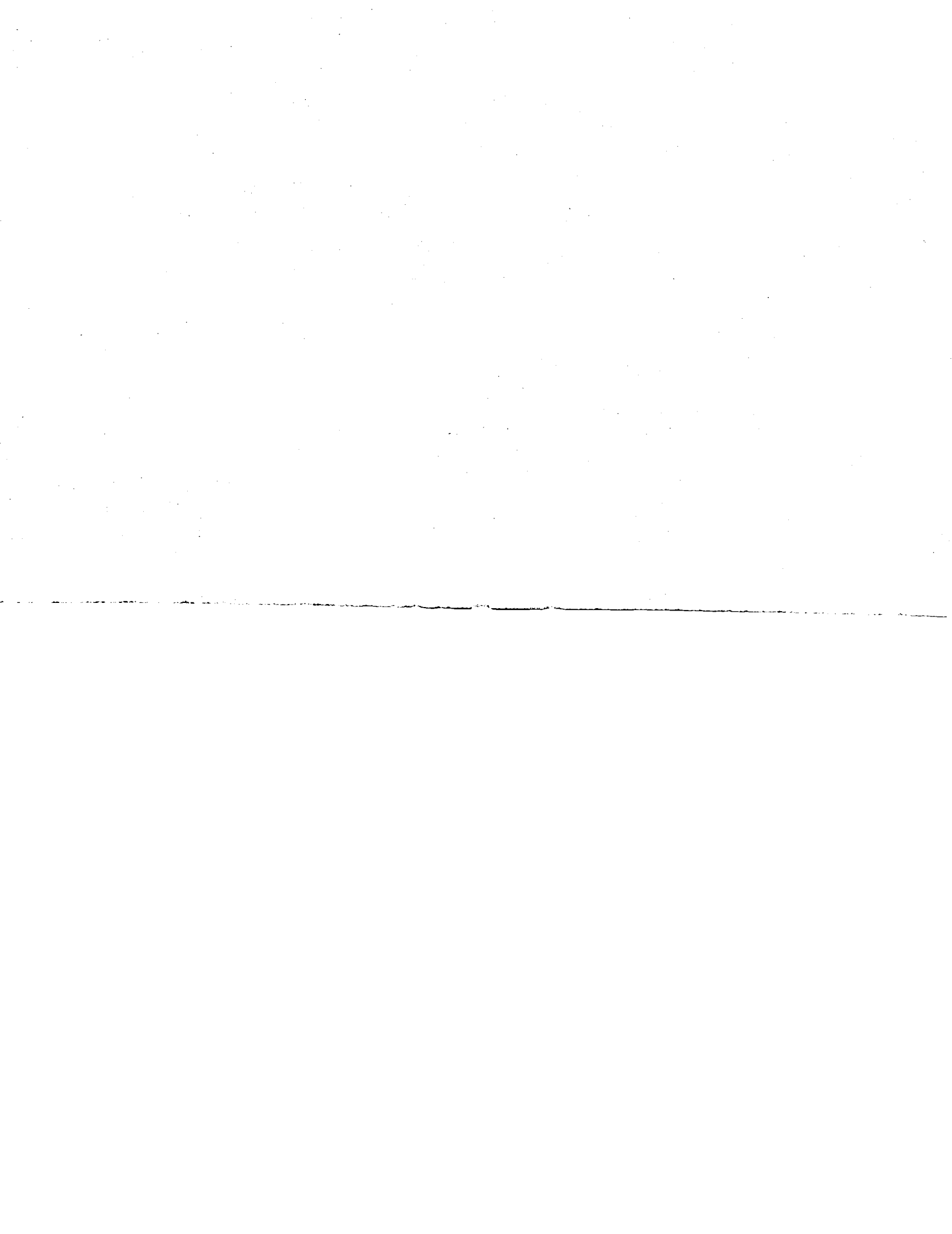
MAJS: /*AUTOMOBILE ENGINES/*COMPUTERIZED SIMULATION/*GAS TURBINE ENGINES

MINS: / ENERGY CONVERSION EFFICIENCY/ MECHANICAL DRIVES/ REAL TIME OPERATION/ TORQUE

ABA: Author

ABS: A hybrid computer simulation of an Advanced Automotive Gas Turbine Powertrain System is reported. The system consists of a gas turbine engine, an automotive drivetrain with four speed automatic transmission, and a control system. Generally, dynamic performance is simulated on the analog portion of the hybrid computer while most of the steady state performance characteristics are calculated to run faster than real time and makes this simulation a useful tool for a variety of analytical studies.

ENTER:



Real-Time Simulation of an Automotive Gas Turbine Using the Hybrid Computer

William Costakis and Walter C. Merrill
National Aeronautics and Space Administration
Lewis Research Center
Cleveland, Ohio 44135

May 1984

Work performed for
U.S. DEPARTMENT OF ENERGY
Conservation and Renewable Energy
Office of Vehicle and Engine R&D
Washington, D.C. 20545
Under Interagency Agreement DE-AI01-77CS51040

N84-26484#

REAL-TIME SIMULATION OF AN AUTOMOTIVE GAS TURBINE USING
THE HYBRID COMPUTER

William Costakis and Walter C. Merrill

National Aeronautics and Space Administration
Lewis Research Center
Cleveland, Ohio 44135

SUMMARY

A hybrid computer simulation of an Advanced Automotive Gas Turbine Powertrain System is reported. The system consists of a gas turbine engine, an automotive drivetrain with four-speed automatic transmission, and a control system. Generally, dynamic performance is simulated on the analog portion of the hybrid computer while most of the steady-state performance characteristics are calculated to run faster than real-time and makes this simulation a useful tool for a variety of analytical studies.

INTRODUCTION

This report describes a hybrid computer simulation of an Advanced Automotive Gas Turbine (AGT) Powertrain System, designated the AGT101. The AGT101 is being developed by the Garrett Turbine Engine Company under NASA contract DEN3-167 sponsored by the Department of Energy (ref. 1). The AGT101 represents a significant advancement in gas turbine state-of-the-art. The engine incorporates ceramic parts to enhance high temperature operation and to provide low cost manufacturing potential for automotive application.

As part of the development of the AGT101 a digital computer simulation was developed to investigate various control strategies and to study engine/drivetrain control dynamic performance. However, since a real-time simulation capability has proven to be very useful and productive tool for controls research, a hybrid computer simulation implementation of the AGT101 was desired. Therefore the digital simulation was converted to a hybrid computer based simulation and is reported herein.

The model, as defined by the engine manufacturer's digital simulation, consists of three basic subsystems: (1) the engine, (2) the drivetrain, and (3) the control. Since the hybrid simulation is to serve as a controls research testbed, the detailed control subsystem supplied by the manufacturer was not required. However, to facilitate the comparison between the hybrid and digital simulations, the control subsystem was included in the hybrid simulation but in a simplified form. These simplifications result in some minor discrepancies between the hybrid and digital simulations, particularly in small transients close to idle speed. However, these discrepancies do not seriously impact the usefulness of the hybrid simulation. Further, dynamic and steady-state comparisons between the hybrid and digital simulations of the engine and drivetrain components are good. These comparisons indicate that the hybrid simulation can be used as a realistic controls testbed facility.

The remainder of the report describes the engine, drivetrain, and control model, the actual hybrid implementation and the results obtained from the hybrid simulation.

SYMBOLS

ALPO	torque converter output angular acceleration
ALPOUT	gearbox output angular acceleration
ALPS1	engine angular acceleration
BETA	VSTC vane angle, deg
CD	aerodynamic drag coefficient
CSLIP	clutch slip, rpm
DNE	speed error, $\Delta NE/NE$
DNERATE	rate of change of speed set point
DTQ/DT4	engine torque correction factor
DT5,TD4	hot side of regenerator temperature correction factor
DWDT4	air flow rate correction factor
EFAXL	rear axle gear efficiency
EFREG	regenerator effectiveness
ENGS	normalized engine speed
EPS,ETR	gear box efficiency
FACC	force available for acceleration
GAMMA	throttle position, deg
GAMI	throttle position integral control, deg
GAMP	throttle position proportional control, deg
GRAXL	rear axle gear ratio
GRTR	transmission gear ratio
GRZ	gear ratio of gear between gearbox and transmission
HPAC	power consumption by accessories, hp
HPACC	power available for acceleration, hp
HPCAR	power at input to gearbox, hp
HPDS	power of the driveshaft, hp
HPLOSS	transmission power loss, hp
HPOTR	power at output of gearbox, hp
HPRL	power required to overcome road load, hp
HPWHL	available power at the wheels, hp
HV	fuel heating valve
IAC	inertia of accessories, lb-ft-sec ²
IGV	compressor inlet guide vane position
IGV1	component of IGV which is a function of engine speed error
IGV2	component of IGV which is a function of GAM
IP12	inertia of planet gear 1 and 2
IP3	inertia of planet gear 3
IR1	inertia transformed to ring gear 1
IR1'	inertia of ring gear 1
IR2	inertia of ring gear 2
IS1	inertia of sun gear 1
ITQC	inertia of input side of torque converter
ITQU	inertia of output side of torque converter and input side of clutch
ITQO	inertia of outside clutch and planet gears 1 and 2
JE	inertia of engine up to torque converter, lb-ft-sec ²
KPB4	VSTC vane control gain
KSET	engine speed set point gain

NC	combustion efficiency
NCTR	speed of torque converter input, rpm
NDS	driveshaft speed, rpm
NE	engine speed, rpm
NECOM	engine speed command, percent
NEP	engine speed, percent
NESET	engine speed set point, percent
NOTR	gearbox output speed, rpm
NP1	number of teeth in planet gear 1
NP2	number of teeth in planet gear 2
NP3	number of teeth in planet gear 3
NR1	number of teeth in ring gear 1
NR2	number of teeth in ring gear 2
NS1	number of teeth in sun gear 1
NS2	number of teeth in sun gear 2
NWHL	wheel speed, rpm
REVM1	revolution per mile of tire
ROL1	rolling friction factor
RN	normal vehicle rolling resistance
SIGMA(σ)	drag coefficient gain on factor
SPIN1	ambient transmission power loss
SPIN2	transmission power loss factor
SPRTIO	ratio of torque converter input speed to accessory design speed
TCKI	torque converter input capacity factor, rpm/ $\sqrt{\text{ft}}$
TCSR	torque converter speed ratio
TCTR	torque converter temperature ratio
TQAC	accessory torque, ft-lb
TQACC	torque available to accelerate vehicle, ft-lb
TQCAR	torque input to gearbox, ft-lb
TQCTR	torque at input of torque converter
TQDS	torque on driveshaft, ft-lb
TQE	unbalance torque accelerating engine, ft-lb
TQOTR	gearbox output torque, ft-lb
TQRL	torque required to overcome road load, ft-lb
TQT	uncorrected engine torque
TQTOT	engine torque, ft-lb
TQWHL	torque to wheels, ft-lb
T3.1	regenerator coldside inlet temperature, °R
T3.6	combustor inlet temperature, °R
T4	turbine inlet temperature, °R
T4ERR	difference between turbine inlet temperature and its set temperature point (T4SET), °R
T4SET	T4 set temperature point, 2960° R
T5.1	regenerator hot side inlet temperature, °R
T5.1ERR	difference between regenerator hot side temperature and its set temperature point, °R
T5.1SET	T5.1 set temperature point, 2460° R
VEL	vehicle speed
VELC	vehicle speed command
VSTC	variable stator torque converter
WAIR	airflow, lb/sec
WAWF	combustor gas flow rate, lb/sec
WF	fuel flow rate, lb/hr
WJ	inertia of transmission through wheels, ft-lb

WO speed of torque converter output, rpm
WT vehicle weight, lb
WTEQ equivalent vehicle weight, lb
WFGAIN governor gain, lb/hr/NEP

SYSTEM MODEL DESCRIPTION

This section describes the model of AGT101 system. The model includes a description of the engine, drivetrain, and control subsystem.

Engine

The engine, shown in figure 1, is a regenerated single-shaft gas turbine engine which is flat-rated at 100 horsepower. The engine consists of a single-stage, 5 to 1 pressure ratio, backward-swept centrifugal compressor and single-stage ceramic radial inflow turbine mounted on a common shaft. Maximum rotor speed for this compressor and turbine configuration is 100 000 rpm. Compressor inlet guide vanes are used to vary engine airflow, and combustor fuel flow is used to vary combustor temperature.

The engine is modeled as shown in figure 2. Model equations are presented in the appendix. The engine model is composed of three parts, the engine performance maps, the regenerator, and the combustor. Engine airflow, torque, and regenerator hot-side and cold-side inlet temperatures are determined as dependent variables from engine performance data maps using turbine inlet temperature, rotor speed, and inlet guide vane positions as independent variables. Combustor inlet (regenerator exhaust) temperature is determined by an energy balance in the regenerator which incorporates the efficiency of heat transfer in the regenerator. Regenerator heat storage is modeled with a regenerator thermal time constant which is dependent upon engine airflow. Combustor operation is modeled by 'curve fit' approximations to the performance of an analytically based, detailed thermodynamic combustor simulation. This simplified combustor model generates the combustor exhaust (turbine inlet) temperature from combustor inlet temperature, air flow, and fuel flow. Finally, engine speed is determined by a conservation of angular momentum equation. The difference between total developed engine torque and the torque required by the drivetrain is used to accelerate the engine rotor.

Drivetrain

For the purposes of this report the drivetrain subsystem includes the gearbox, the transmission, and important physical characteristics of the vehicle. The gearbox is a split path differential design accepting power directly from the engine. Power is split in the differential planetary gears with a portion going directly to the transmission. The remaining power goes to the variable stator torque converter (VSTC). The VSTC provides a variable speed ratio output that is fed back to the planetary carrier and combines with the power delivered to the transmission. The transmission is the Ford four-speed Automatic Overdrive (AOD) production transmission. The transmission model consists of four forward gears. Reverse gearing is not considered in this simulation. Shifting logic is a function of a vehicle velocity. The

transmission couples the output power of the gearbox with the vehicle. The vehicle drivetrain subsystem is composed of the driveshaft, the differential, the rear axle of the car, and the wheels. Vehicle weight, inertia, and road load characteristics are also included in the simulation. The subject vehicle of this simulation is a 3000-pound vehicle of the Ford Fairmont class.

The drivetrain model is also shown in figure 2 with model equations given in the appendix. Basic inputs to the drivetrain are the VSTC control variable, BETA, and engine rotor speed. The outputs of the drivetrain model are vehicle required torque as well as important internal drivetrain variables such as vehicle velocity.

The VSTC vane angle, BETA, along with a calculated VSTC speed ratio are used as inputs to performance maps (obtained from test data) of the VSTC. The outputs are VSTC torque ratio and VSTC capacity factor. These outputs along with efficiency of the gearbox, transmission, and axle, the gear ratio of the transmission, vehicle velocity, and accessory load are used to calculate the vehicle required torque. Vehicle velocity is calculated from a conservation of angular momentum equation. The difference between the torque applied to the wheel and the torque due to the road load accelerates the vehicle. Road load is found as a function of vehicle weight, velocity, and grade of the road.

Control

The control model is shown schematically in figure 2 and the model equations are given in the appendix. Basically, the control has three independent or manipulated variables, compressor inlet guide vane position (IGV), fuel flow rate (WF), and VSTC vane angle (BETA). Inlet guide vane position is used to optimize compressor performance with respect to shaft speed and is scheduled open-loop as a function of commanded rotor speed error and the throttle pedal angle (GAMMA). The fuel flow rate is determined by a closed-loop proportional plus integral control on engine rotor speed. Command engine speed is a direct function of GAMMA. Finally, VSTC vane angle (BETA) is determined by closed-loop proportional control on either combustor exhaust temperature or turbine exhaust temperature. One, or the other, of these two temperatures is controlled to its respective constant, predetermined setpoint value. The maximum of the two temperature errors (setpoint minus actual) determines which loop is selected as the active control loop.

HYBRID SIMULATION

The equations describing the AGT101 power train system were implemented on the Lewis Research Center's PACER600 hybrid computing system. This system consists of an EAI PACER 100 digital computer, a model 680 analog computer and a model 681 analog computer.

The digital computer was used primarily to perform the generation of the engine's performance maps and the torque converter maps. The digital computer was also used to implement the shifting logic and to calculate the ambient transmission power loss (SPIN1) and the transmission power loss factor (SPIN2). The scaled-fraction variables and the digital function generator programs MAP and MAPL, used in the digital programs, are discussed in reference 2.

The remaining calculations were performed on the analog computer. The analog computer performed such computations as summing, integration with respect to time, multiplication, univariable function generation, and so forth, which are suitable to analog computing. Strip-chart recorders were used to continuously monitor and record the computed variables.

RESULTS AND DISCUSSION

The intent of the hybrid simulation was to demonstrate the feasibility of using the hybrid computer to simulate, in real-time, AGT101 performance. The simulation then could be used as a test bed for evaluating various research control strategies.

The basis for the hybrid simulation was the digital simulation provided by the engine manufacturer. Some digital simulation results are presented for comparison with hybrid simulation results to establish validity of the hybrid results.

A comparison between steady-state hybrid and digital simulation results is presented in Table I. Results for throttle settings of 20°, 40° and 50° are shown in Table I. Steady-state results for both the digital and hybrid simulations were obtained by first increasing the throttle from 0° to the final desired throttle setting in a step-wise fashion, and then allowing the simulation sufficient time to reach its steady-state point.

Twenty-three engine variables are compared in Table I. For every one of these variables the hybrid results compared well with the digital results.

The transient data are responses of selected engine variables to a step throttle command under zero road grade conditions. Prior to the throttle step input, the simulation was set at the idle ($\text{GAMMA} = 0$) initial conditions. Transient data from the hybrid simulations were obtained for throttle command step inputs from 0° to 20° and 40°, with the results presented in figures 3 and 4. Transient responses of eleven engine variables, using the digital simulation, are presented in figures 5 and 6. The responses are for throttle step inputs of 20° and 40°. A comparison between the hybrid and the digital simulation dynamic responses shows that they are quite similar. Figures 3 and 5 which are the results of the 20° throttle step input for the hybrid and digital simulations, respectively, indicate that the transmission shifted through the first three gears only, and the vehicle attained its final steady-state velocity in the third gear. The results for the 40° throttle step input, shown in figure 4 for the hybrid simulation, show that the transmission shifts through all four gears and the vehicle attains its final steady-state velocity in the fourth gear. The digital simulation results shown in figure 6 are similar.

Also the results in figures 3 and 4 indicate that the smaller the throttle step input the longer it takes to shift from one gear to the next. Consequently, the larger the step input the faster the vehicle attained its final steady-state velocity. The digital simulation results showed the same trend.

The only difference of any significance between the hybrid and the digital simulation with regards to the transmission was in the shift point

timing. The hybrid simulation used somewhat less time between shift points than the digital simulation. This difference, however, was expected since the actuator dynamics associated with the IGV's and VSTC's were not included in the hybrid simulation.

The other area where the simulation differed was at an idle or near idle condition. In the digital simulation with the transmission in first gear, throttle command at zero degrees and zero road grade conditions, the vehicle attained a steady speed of 0.26 miles per hour. Prior to the throttle command step input in the hybrid simulation, the vehicle attained a steady velocity of 15.68 miles per hour. This can be explained by the fact that hybrid simulation did not include the detailed control employed in the digital simulation. As an example, the hybrid simulation did not provide for the reduction of fuel flow when T4 and T5.1 exceeded the over temperature limits. It also did not provide for integration of IGV's to open position if either T5.1 or T4 exceeded their set points. The net result was that the hybrid simulation would run richer at idle and consequently would stabilize at a higher vehicle velocity than the digital. Since this was a control system related discrepancy, it has no significant effect on the evaluation of the hybrid simulation.

The dynamic response of all the torques, the position of the VSTC vanes (BETA), percent engine speed (NEP), vehicle velocity (VEL) and fuel flow (WFL) to a 20° and 40° throttle command shown in figures 3 and 4, respectively, compared well with the digital simulation results shown in figures 5 and 6.

The hybrid simulation compressor inlet guide vane (IGV) position dynamic response shown in figures 3 and 4 varied somewhat from the digital simulation response shown in figures 5(b) and 6(b). However, since there was significant control logic in the digital simulation that affected the IGV's directly which did not exist in the hybrid, this small difference in the IGV response was not considered important.

SUMMARY OF RESULTS

This report describes a real-time hybrid computer simulation of the AGT101 automatic gas turbine powertrain system. The AGT101 real-time simulation was modeled after the manufacturer's digital simulation. Since the real-time simulation was intended to serve as a control research testbed, the detailed control supplied by the manufacturer's digital simulation was not included. Steady-state data are presented for three throttle positions at zero road grade conditions. Transient data are presented in the form of engine variable responses to two throttle step inputs under zero road grade conditions. Both steady state and transient data of the real-time simulation compared well with the digital simulation data. Differences between the two sets of data at idle or near idle condition were due to the exclusion of the control supplied with the digital simulations from the real-time simulation. The real-time simulation shifted somewhat faster than the digital simulation because the actuator dynamics associated with the IGV's and VSTC vanes were not included in the simulation.

The simulation structure described in this report resulted in stable real-time operation.

APPENDIX - EQUATIONS

I. Simulated Driver Commands:

$$\text{GAMMA} = \text{GAMI} + \text{GAMP}$$

$$\text{GAMP} = \text{KV1} \Delta \text{VEL}$$

$$\text{GAMI} = \text{KV2} \Delta \text{VEL} dt$$

$$\Delta \text{VEL} = \text{VELC} - \text{VEL}$$

II. IGV Control:

$$\text{IGV} = \text{IGV1} + \text{IGV2}$$

$$\text{IGV1} = f(\text{DNE}) = -\text{DNE}$$

$$\text{IGV2} = f(\text{GAMMA})$$

$$\text{IGVL} = \frac{\text{IGV}}{1 + \tau_{\text{IGV}} S} \quad \tau_{\text{IGV}} = 0.01$$

III. Fuel Speed Control:

$$\text{NECOM} = f(\text{GAMMA})$$

$$\text{WF} = \text{WFGAIN}(\text{NESET} - \text{NEP}) \quad \text{WFGAIN} = 3$$

$$\text{NESET} = \frac{\text{KSET}}{S} (\text{DNERATE}) \quad \text{KSET} = 4$$

$$\text{DNERATE} = f(\text{DNE})$$

$$\text{DNE} = \frac{\text{NECOM} - \text{NEP}}{\text{NEP}}$$

$$\text{WFL} = \frac{\text{WF}}{1 + \tau_F S} \quad \tau_F = 0.01$$

IV. Engine Maps

Engine air flow:

$$\text{WAIRM} = f(\text{NEP}, \text{IGVL})$$

$$\text{WAIRC} = \text{WAIRM} - \text{DWDT4}(\text{T4} - 2960)$$

$$\text{DWDT4} = \frac{7.5}{10^5} - \frac{\text{IGVL}}{10^6}$$

$$\text{WAIRL} = \frac{\text{WAIRC}}{1 + \tau_A S} \quad \tau_A = 1.01$$

Engine torque:

$$TQT = f(NEP, IGV_L)$$

$$DTQDT4 = f(NEP, IGV_L)$$

$$TQTOT = TQT + DTQDT4 \quad \frac{T_4 - 2760}{1000} - 5 \times 10^{-5} \left| (T_4 - 2760) \right|$$

Regenerator temperatures:

$$T_{3.1} = f(NEP, IGV_L)$$

$$T_{5.1M} = f(NEP, IGV_L)$$

$$DT_{5.1D4} = 0.77 + 0.006170NEP - (0.613642 \times 10^{-4} NEP^2)$$

$$T_{5.1} = T_{5.1M} + DT_{5.1D4}(T_4 - 2960)$$

V. Regenerator

$$EFREG = 0.98525 - 0.01074WAIRL - 0.1004WAIRL^2 + 0.03617WAIRL^3$$

$$T_{3.6} = T_{3.1} + EFREG(T_{5.1} - T_{3.1})$$

$$T_{3.6L} = \frac{T_{3.6}}{1 + \tau_{REG}^S}$$

$$\tau_{REG} = 0.33 + \frac{4.25}{WAIRL}$$

VI. Combustor

$$T_4 = \frac{[(ECOMB)^2 + DCOMB]^{0.5} - ECOMB}{0.224 \times 10^4 WAWF}$$

$$WAWF = WAIRL + \frac{WFL}{3600}$$

$$ACOMB = \frac{1}{0.664} \left(0.65 + \frac{WFL}{3600WAIRL} \right)$$

$$BCOMB = WAIRL (0.24 + 0.61 \times 10^{-6} Y) (T_{3.6L} - 536.7)$$

$$CCOMB = \eta_C(HV) \frac{WFL}{3600}$$

$$DCOMB = 0.448 \times 10^{-4} WAWF \left(\frac{BCOMB + CCOMB + 129.3 WAWF}{ACOMB} \right)$$

$$ECOMB = 0.2355 WAWF$$

$$Y = (T3.6L)^{1.35}$$

VII. VSTC Vane Control

$$T5.1L = \frac{T5.1}{1 + \tau_{TH}S} \quad \tau_{TH} = 4$$

$$T5.1LL = \frac{1 + \tau_1 S}{1 + \tau_2 S} T5.1L \quad \begin{aligned} \tau_1 &= 4 \\ \tau_2 &= 0.8 \end{aligned}$$

$$T5.1ERR = T5.1LL - T5.1SET \quad T5.1SET = 2460^\circ R$$

$$T4L = \frac{T4}{1 + \tau_{TH}S}$$

$$T4LL = \frac{1 + \tau_1 S}{1 + \tau_2 S} T4L$$

$$T4ERR = T4LL - T4SET \quad T4SET = 2960^\circ R$$

$$\text{BETA} = 84 + \text{KPB4}(TERR) \quad \text{KPB4} = 0.8$$

$$\text{TERR} = \text{Max}(T5.1ERR, T4ERR)$$

VIII. Gear Box System

$$\text{NOTR} = \text{NDS}(\text{GRTR})(\text{GRZ}) \quad \text{GRZ} = 1.0405$$

$$\text{NDS} = \text{NWHL}(\text{GRAXL}) \quad \text{GRAXL} = 2.730$$

$$\text{NWHL} = \frac{\text{REVMI}}{60} (\text{VEL})$$

$$\text{GRTR} = f(\text{GEAR})$$

$$\text{HPOTR} = \frac{\text{TQOTR(NOTR)}}{5252}$$

$$\begin{aligned} \text{TQOTR} = E6 \left[(F6)(\text{TQCAR}) - G6(\text{ALPS1}) + IP12(\text{ALPOUT}) \left(\frac{NS1}{NP1} \right) \right] \\ + \text{TQCTR}(\text{TCTR}) - \text{ALPO}(\text{ITQU}) \end{aligned}$$

$$\text{EPS} = \text{ETR}$$

$$\text{ALPS1} = \frac{2\pi}{60} \frac{dNE}{dt} = \frac{2\pi(12)(9.5493)}{60(JE)} \text{TQE}$$

$$\text{ALPOUT} = \frac{2\pi}{60} \frac{\text{REVMI}}{60} (\text{GRAXL})(\text{GRTR})(\text{GRZ}) \frac{d\text{VEL}}{dt}$$

$$A_6 = \left(\frac{N_1}{N_1} \right)^2 (I_{P12})(EPS)^2 = \frac{2.3192}{10^5} EPS^2$$

$$B_6 = \left[\frac{N_1(N_2)}{N_1(N_1)} \right]^2 = 0.06948$$

$$C_6 = 1 + \frac{N_1(N_1)}{N_1(N_2)} = 15.8571$$

$$D_6 = \left[\frac{N_2(N_1)(N_2)}{N_1(N_1)(N_2)} \right] \left(\frac{1}{EPS} \right)^6 = \frac{0.05256}{(EPS)^6}$$

$$E_6 = \frac{N_1(N_1)}{N_1(N_2)} = 0.12771$$

$$F_6 = N_2(EPS) + (N_1)(EPS)^2 = (42 + 96EPS)EPS$$

$$G_6 = N_1(I_{S1})(EPS)^2 + N_2(I_{S1})EPS + \left(\frac{I_{P12}}{N_1} \right) (N_1)^2 = 0.00229$$

where

$$I_{S1} = I_{P3} = I_{AC} = I_{R2} = 0 \quad ITQC = 0.075$$

$$I_{P12} = 0.0004416 \quad ITQU = 0.0104166$$

$$I_{R1'} = 0.036583 \quad ITQO = 0.008125$$

$$I_{R1} = I_{R1'} + I_{P3} \left(\frac{N_2}{N_3} \right)^2 + (I_{R2} + I_{AC} + ITQC) \left(\frac{N_2}{N_2} \right)^2$$

and

$$N_1 = 22 \quad N_1 = 96 \quad N_2 = 42 \quad N_1 = 143$$

$$N_2 = 171 \quad N_3 = 23 \quad N_2 = 219$$

Clutch Slip:

For NEP > 56 or GAM > 1

$$CSLIP = \left[\frac{1}{ASR}(NE) - \left(\frac{CSR}{(ASR)(BSR)} \right) (NOTR) \right] TCSR - NOTR$$

$$ASR = \frac{N_1(N_1)(N_2)}{N_1(N_2)(N_2)}$$

$$BSR = N_1(N_2)$$

$$CSR = (N_1)(N_2) + (N_1)(N_1)$$

For NEP \leq 56 or GAM \leq 1

CSLIP = 0

Efficiency:

$$ETR = AGE + BGE(HPCAR) + CGE(HPCAR)^2 + DGE(HPCAR)^3$$

$$HPCAR = \frac{TQCAR(NE)}{5252}$$

$$AGE = 0.97015 + ENGS(0.0307903 - 0.07365 ENGS)$$

$$BGE = 5.2315 \times 10^{-4} + ENGS(2.15 \times 10^{-4} + 1.0562 \times 10^{-3} ENGS)$$

$$CGE = 3.68359 \times 10^{-6} - ENGS(1.20716 \times 10^{-5} + 2.14907 \times 10^{-6} ENGS)$$

$$DGE = 7.47466 \times 10^{-9} + ENGS(6.856 \times 10^{-8} - 1.5756 \times 10^{-8} ENGS)$$

$$ENGS = \frac{NE}{10^5}$$

Torque Converter:

$$TCSR = \frac{ASR(BSR)(NOTR + CSLIPL)}{BSR(NE) - NOTR(CSR)}$$

$$NCTR = \frac{W_0}{TCSR}$$

$$W_0 = NOTR + CSLIPL$$

$$TCKI = f(TCSR, \beta)$$

$$TQCTR = (NCTR/TCKI)^2$$

$$TCTR = f(TCSR, \beta)$$

$$HPCTR = \frac{NCTR(TQCTR)}{5252}$$

IX. Accessory Torque and Power Consumption

$$TQAC = 5252(HPAC/NCTR)$$

$$HPAC = 2.342(SPRATIO)^{1.0138}$$

$$SPRATIO = \text{MAX}(0.001, SPRATIO')$$

$$SPRATIO' = NCTR/4000$$

X. Engine Acceleration Torque and Speed

$$TQE = TQTOT - TQCAR$$

$$\frac{dNE}{dt} = \frac{114.6}{JE} TQE \quad JE = 0.0052$$

$$NEP = \frac{NE}{10^3}$$

$$TQCAR = \left[IS1 + A6 + B6 \left(\frac{IR1}{EPS^6} \right) \right] ALPS1 - \left[A6 + B6(C6) \left(\frac{IR1}{EPS^6} \right) \right] ALPOUT + (TQAC + TQCTR) D6$$

XI. Transmission Efficiency

$$HPLOSS = SPIN1 + SPIN2(TQDS)$$

$$HPLOSS = \text{Max}(0, HPLOSS)$$

For gear 1:

$$SPIN1 = 0.09459 - 0.08389 \times 10^{-3} NDS + 5.168 \times 10^{-6} NDS^2 - 4.020 \times 10^{-9} NDS^3 + 1.295 \times 10^{-12} NDS^4$$

$$SPIN2 = 0.0003162 + 0.0247 \times 10^{-3} NDS - 0.02772 \times 10^{-6} NDS^2 + 0.01043 \times 10^{-9} NDS^3 - 0.0002181 \times 10^{-12} NDS^4$$

For gear 2:

$$SPIN1 = 0.05734 + 0.4648 \times 10^{-3} NDS + 0.7247 \times 10^{-6} NDS^2 - 0.1023 \times 10^{-9} NDS^3 + 0.01740 \times 10^{-12} NDS^4$$

$$SPIN2 = 0.0004343 + 0.01310 \times 10^{-3} NDS - 0.009127 \times 10^{-6} NDS^2 + 0.002259 \times 10^{-9} NDS^3 + 0.0000754 \times 10^{-12} NDS^4$$

For gear 3:

$$SPIN1 = -0.05786 + 0.6550 \times 10^{-3} NDS + 0.02488 \times 10^{-6} NDS^2 + 0.06789 \times 10^{-9} NDS^3 - 0.007325 \times 10^{-12} NDS^4$$

$$SPIN2 = -0.000167 + 0.008048 \times 10^{-3} NDS - 0.000706 \times 10^{-6} NDS^2 + 0.00193 \times 10^{-9} NDS^3 - 0.0001554 \times 10^{-12} NDS^4$$

For gear 4:

$$SPIN1 = -0.03036 + 0.4248 \times 10^{-3} NDS + 0.0214 \times 10^{-6} NDS^2 + 0.01863 \times 10^{-9} NDS^3 - 0.001192 \times 10^{-12} NDS^4$$

$$SPIN2 = -0.0010137 + 0.01585 \times 10^{-3} NDS - 0.005401 \times 10^{-6} NDS^2 + 0.001154 \times 10^{-9} NDS^3 - 0.00005956 \times 10^{-12} NDS^4$$

For NDS < 10, HPLOSS = 0

XII. Axle Efficiency

$$EFAXL = 0.0785 + 0.505624CR - 0.098384CR^2 + 0.00648856CR^3$$

$$CR = \log \left(\frac{5252 \text{ HPDS}}{\text{NWHL}} \right)$$

$$0 \leq CR \leq 5.983$$

$$\text{HPDS} \geq 0.1 \times 10^{-4}$$

XIII. Wheel and Drive Shaft

$$TQWHL = GRAXL(EFAXL)(TQDS) = \frac{5252 \text{ HPWHL}}{\text{NWHL}}$$

$$TQDS = \frac{5252(\text{HPDS})}{\text{NDS}}$$

$$\text{HPDS} = \text{HPOTR} - \text{HPLOSS}$$

$$\text{HPWHL} = \frac{TQDS(\text{NDS})}{5252} = \text{HPDS}(EFAXL)$$

XIV. Road Load

$$\begin{aligned} \text{HPRL} = & \left\{ \left(\frac{\text{WT}}{\text{RN}} \right) [1.0 + \text{ROL1}(\text{VEL})] + 0.002557(\sigma)(CD)(AFNT)(\text{VEL})^2 \right\} \left(\frac{\text{VEL}}{375} \right) \\ & + \text{WT(GRADE)} \left(\frac{\text{VEL}}{375} \right) \end{aligned}$$

XV. Vehicle Velocity

$$\frac{d\text{VEL}}{dt} = \frac{21.937(\text{FACC})}{\text{WTEQ}}$$

$$\text{FACC} = \frac{\text{TQACC}}{\text{RADIUS}}$$

$$\text{WTEQ} = \text{WT} + \frac{322\text{WJ}}{12(\text{RADIUS})^2}$$

$$\text{RADIUS} = \frac{5280}{2\pi \text{ REVMI}}$$

$$\text{TQACC} = \frac{5252(\text{HPACC})}{\text{NWHL}}$$

$$\text{HPACC} = \text{HPWHL} - \text{HPRL}$$

REFERENCES

1. Advanced Gas Turbine (AGT) Powertrain System Development for Automotive Applications. (Garrett No. 31-3725(3), Garrett Turbine Engine Co.; NASA Contract DEN3-167.) DOE/NASA/0167-8113, NASA CR-167901, 1981.
2. Bruton, William M.; and Cwynar, David S.: Lewis Hybrid Computing System-Users Manual. NASA TM-79111, 1979.

TABLE I. - COMPARISON OF STEADY STATE HYBRID AND
DIGITAL SIMULATION RESULTS

(a) Throttle setting, 20° (b) Throttle setting, 40° (c) Throttle setting, 50°

Engine vari- ables	Digital simu- lation	Hybrid simu- lation	Engine vari- ables	Digital simu- lation	Hybrid simu- lation	Engine vari- ables	Digital simu- lation	Hybrid simu- lation
GAMMA	20°	20°	GAMMA	40°	40°	GAMMA	50°	50°
IGV	45.00	45.02	IGV	41.67	41.62	IGV	39.8	39.9
BETA	69.01	68.18	BETA	74.82	78.04	BETA	50.22	50.39
GEAR	3	3	GEAR	4	4	GEAR	4	4
NEP	63.00	62.93	NEP	67.45	67.36	NEP	76.04	75.92
VEL	41.30	41.32	VEL	49.85	49.84	VEL	70.08	70.07
WAIRL	0.2756	0.2737	WAIRL	0.3240	0.3231	WAIRL	0.4131	0.4130
WFL	5.008	4.050	WFL	7.325	6.985	WFL	12.53	11.31
T4	2688	2716	T4	2769	2792	T4	2903	2856
T5.1	2417	2442	T5.1	2437	2457	T5.1	2468	2427
T3.6L	2380	2425	T3.6L	2389	2413	T3.6L	2401	2374
TQCAR	1.144	1.148	TQCAR	1.649	1.610	TQCAR	2.620	2.541
TQACC	15.55	15.40	TQACC	12.26	11.00	TQACC	12.106	2.200
TQDS	32.10	35.10	TQDS	38.05	30.00	TQDS	60.42	60.00
TQOTR	35.06	35.10	TQOTR	61.22	54.00	TQOTR	95.22	90.00
NOTR	1676	1675	NOTR	1349	1348	NOTR	1897	1896
HPRL	7.627	8.635	HPRL	11.78	12.93	HPRL	24.84	29.37
TQWHL	83.46	92.00	TQWHL	99.16	80.00	TQWHL	158.2	160.0
TCTR	1.024	1.017	TCTR	1.379	1.325	TCTR	1.203	1.198
TCKI	487.1	485.0	TCKI	492.4	530.0	TCKI	373.2	380.0
TCSR	0.8752	0.8797	TCSR	0.5573	0.5603	TCSR	0.7851	0.7901
NCTR	1915	1904	NCTR	2420	2406	NCTR	2416	2402
EFAXL	0.9524	0.9529	EFAXL	0.9547	0.9505	EFAXL	0.9590	0.9589

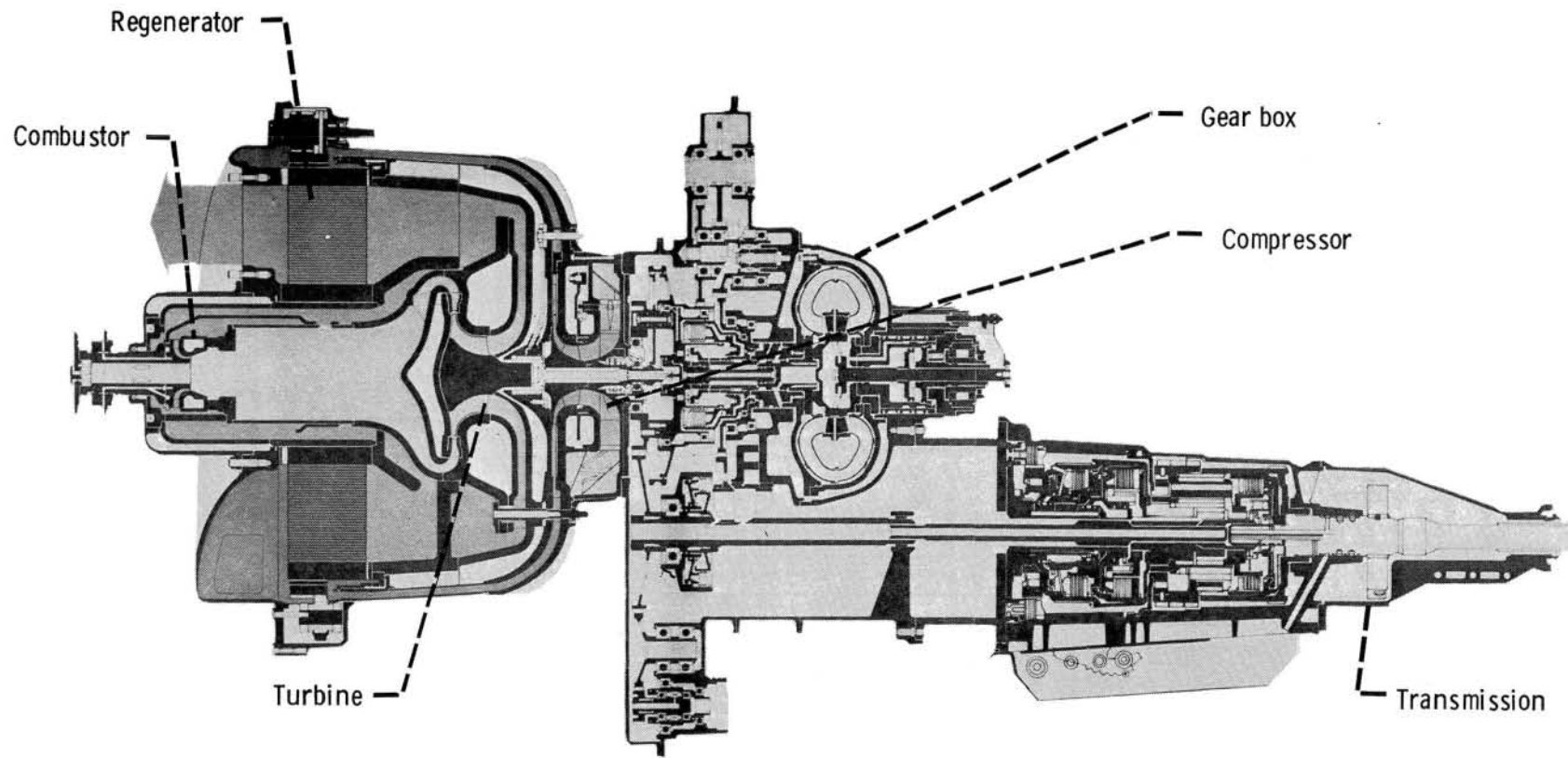


Figure 1. - Advanced gas turbine powertrain.

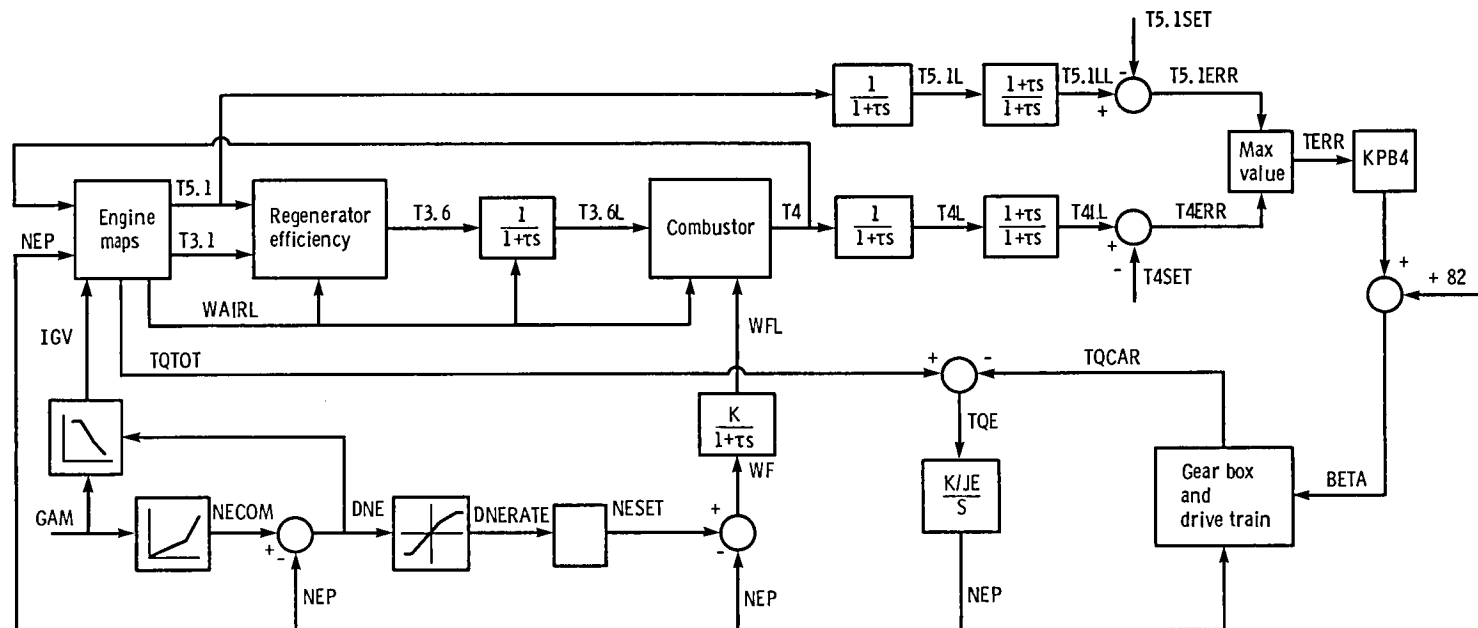


Figure 2. - Simplified block diagram of AGT101.

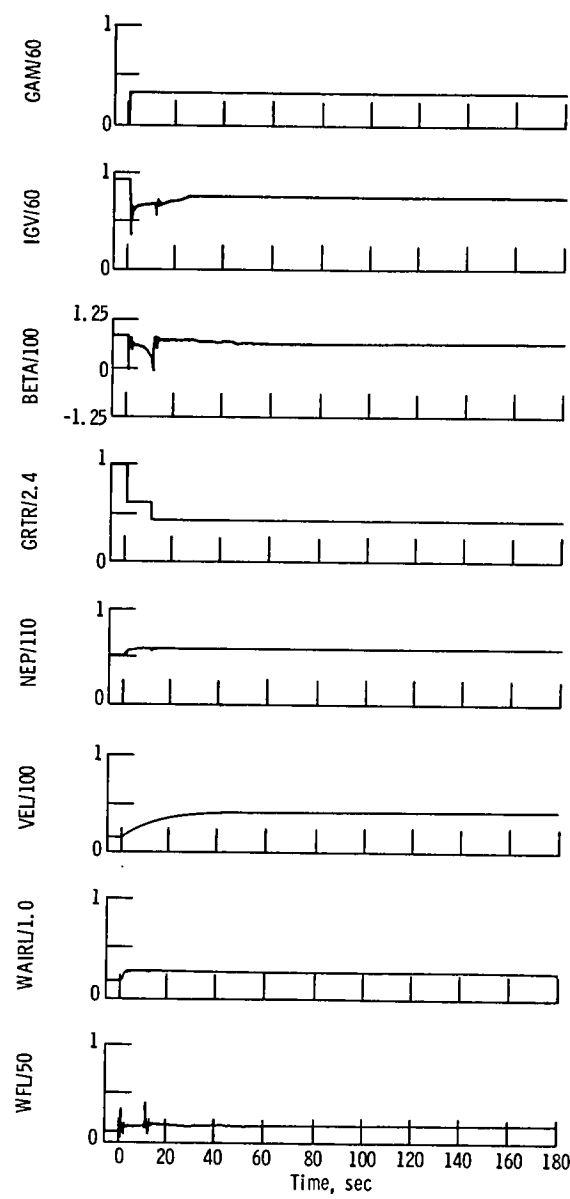


Figure 3. - Engine response to throttle step command from 0° to 20° .

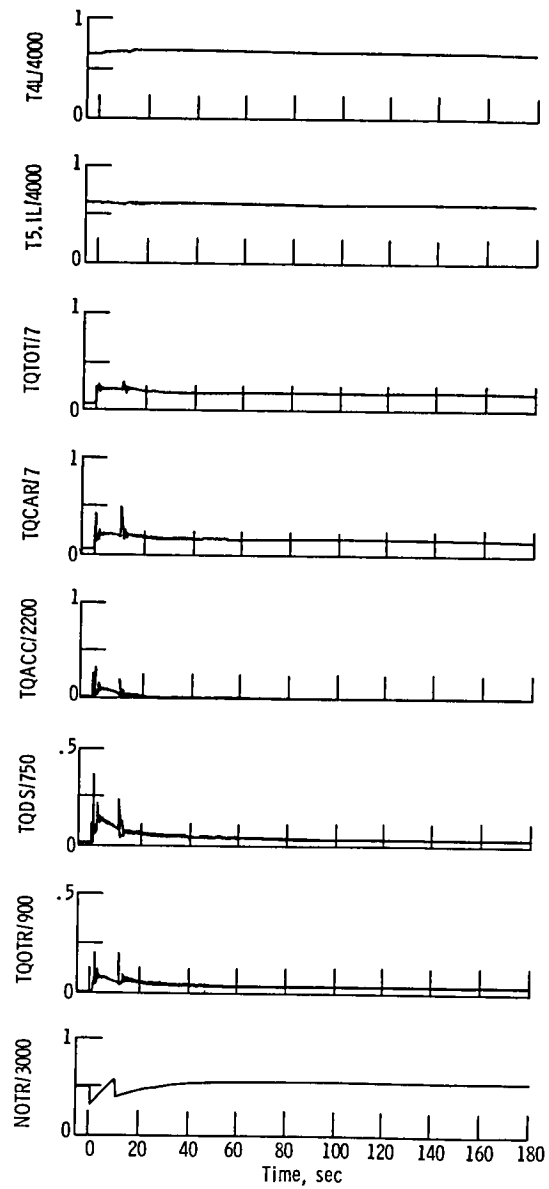


Figure 3. - Concluded.

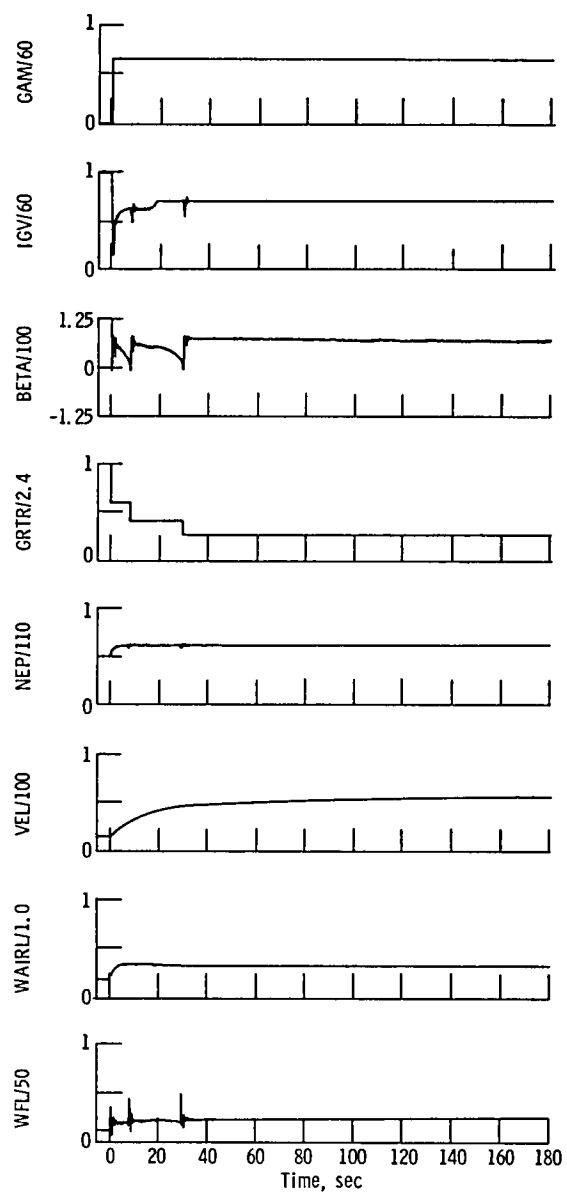


Figure 4. - Engine response to throttle step command from 0° to 40° .

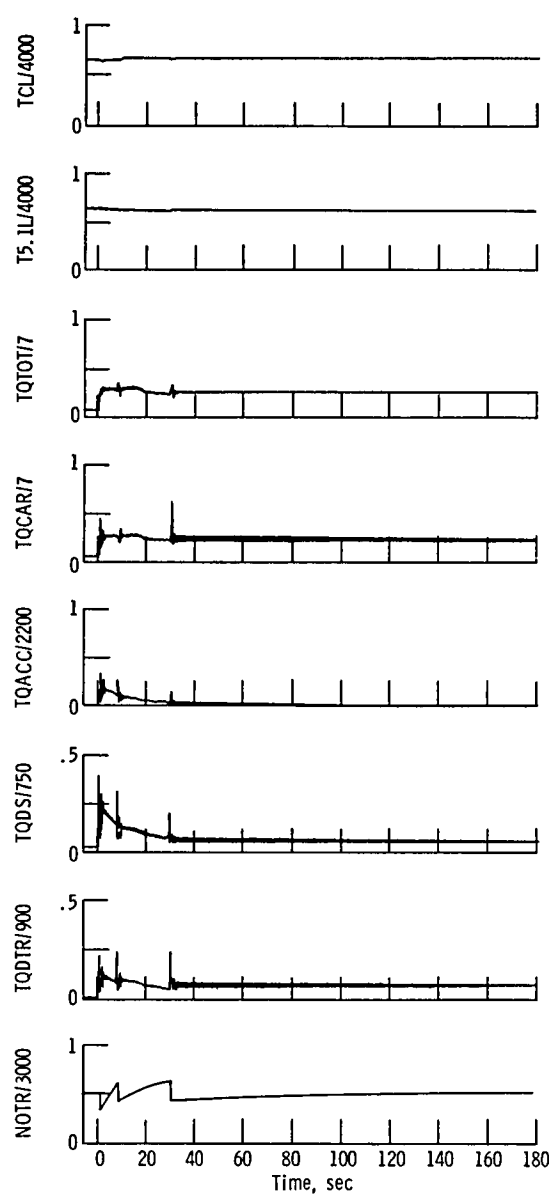


Figure 4. - Concluded.

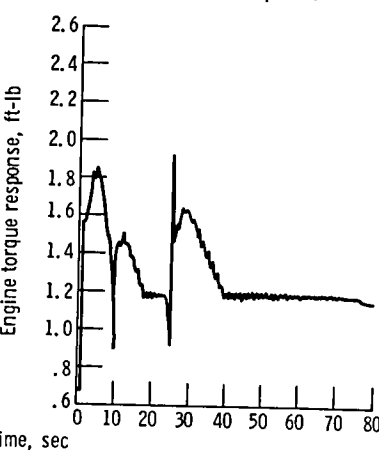
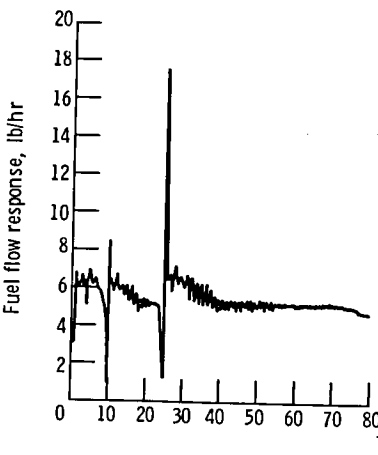
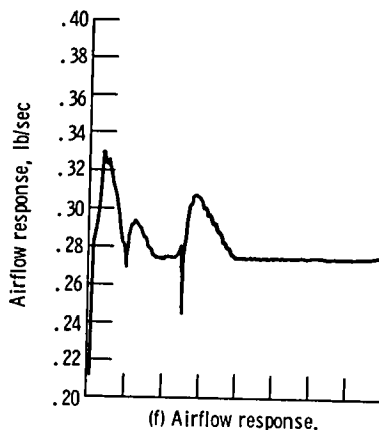
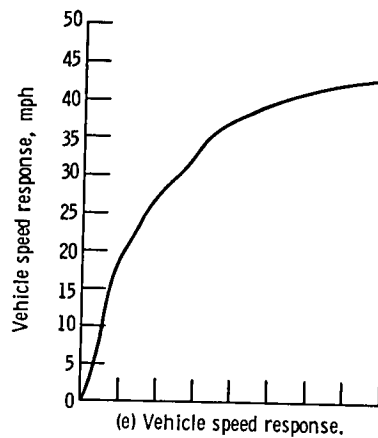
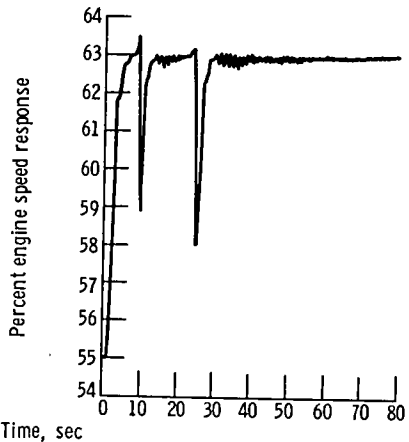
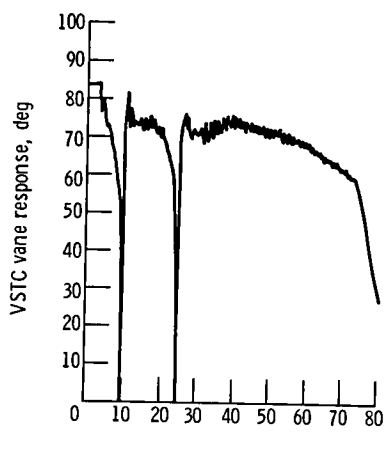
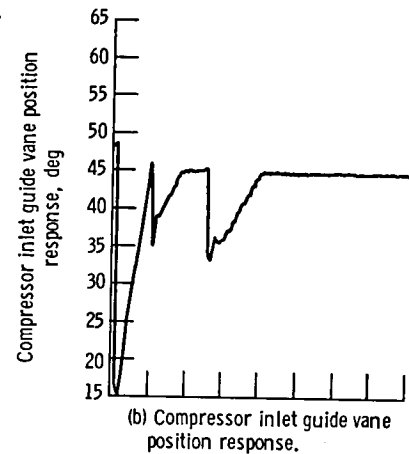
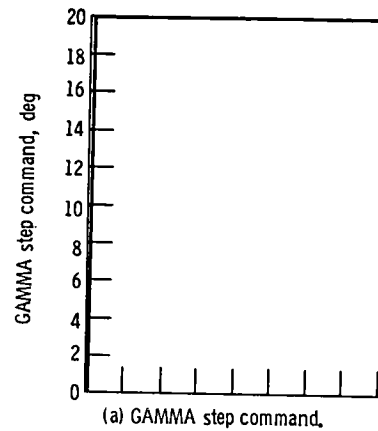


Figure 5. - Digital simulation dynamic results ; GAMMA step command from 0° to 20° .

Figure 5. - Continued.

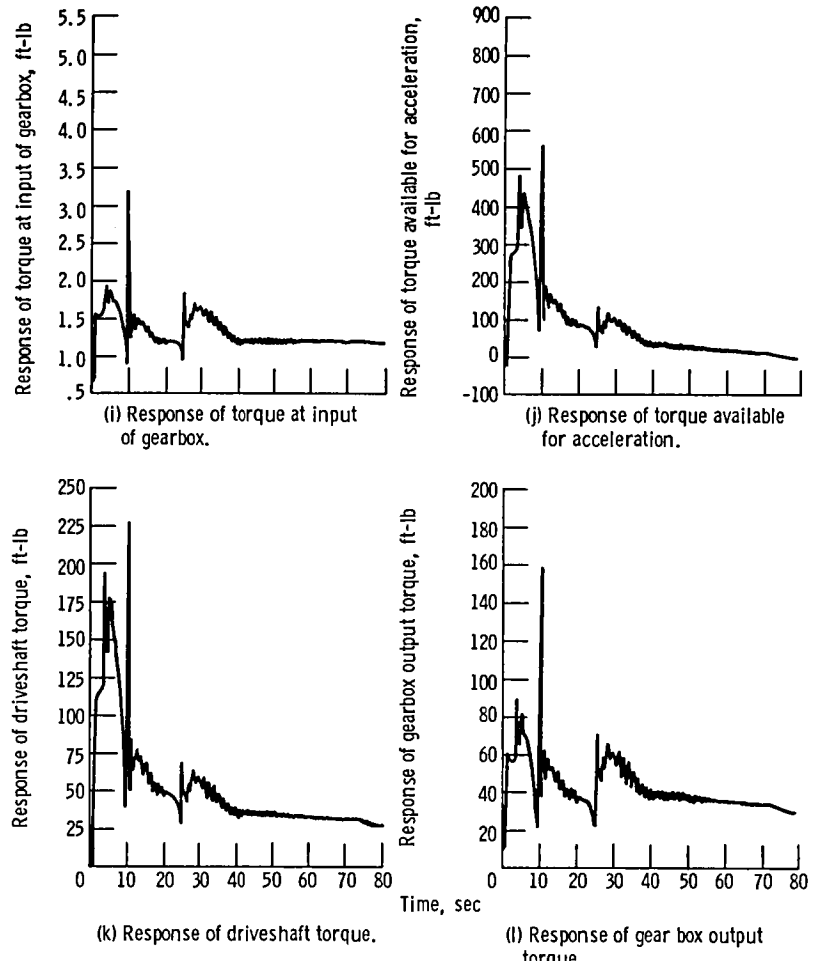


Figure 5. - Concluded.

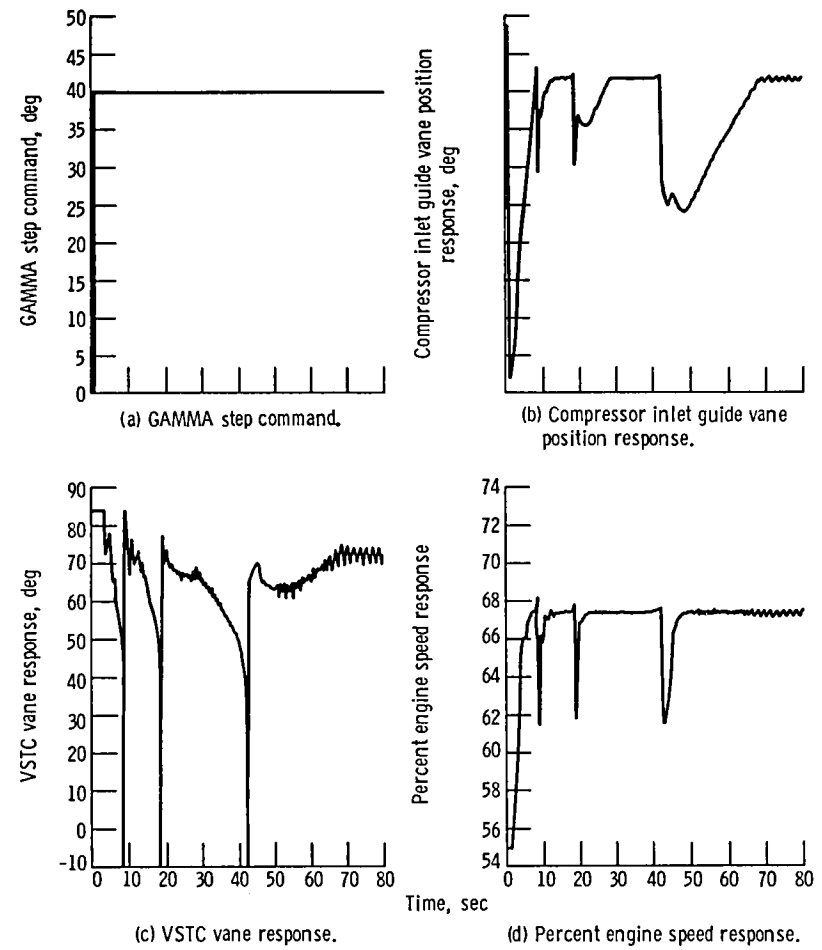


Figure 6. - Digital simulation dynamic results; GAMMA step command from 0° to 40° .

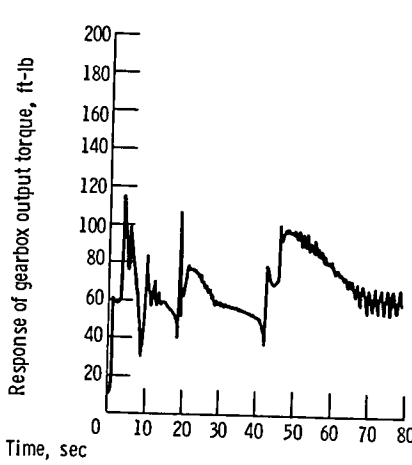
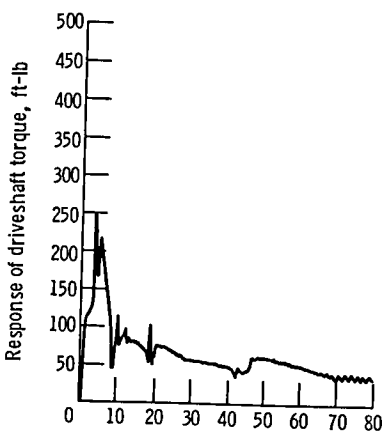
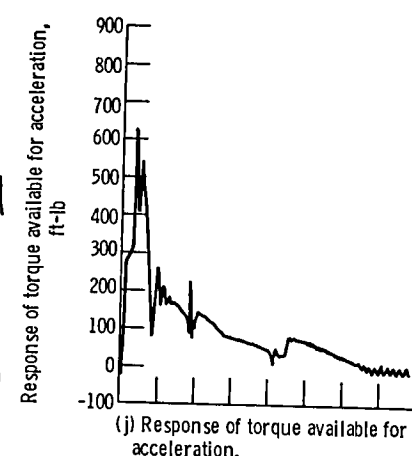
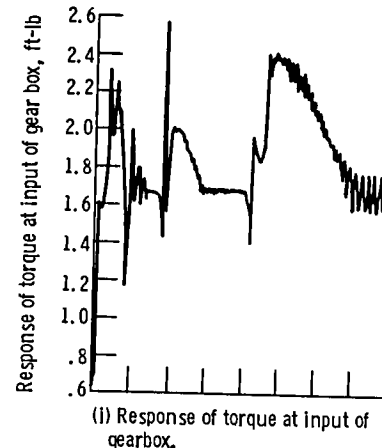
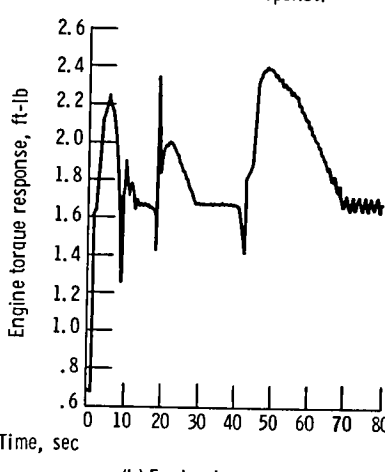
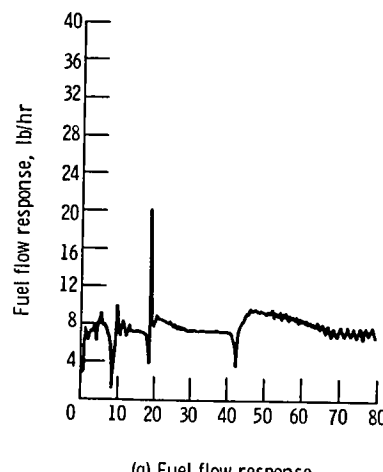
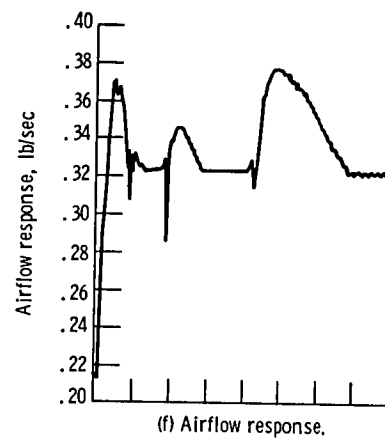
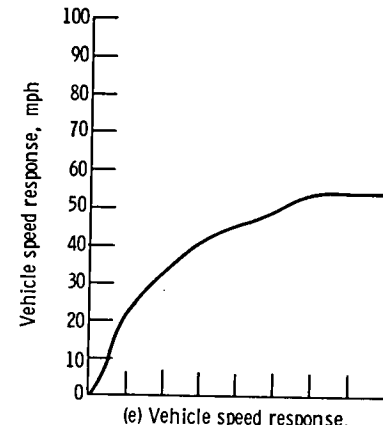
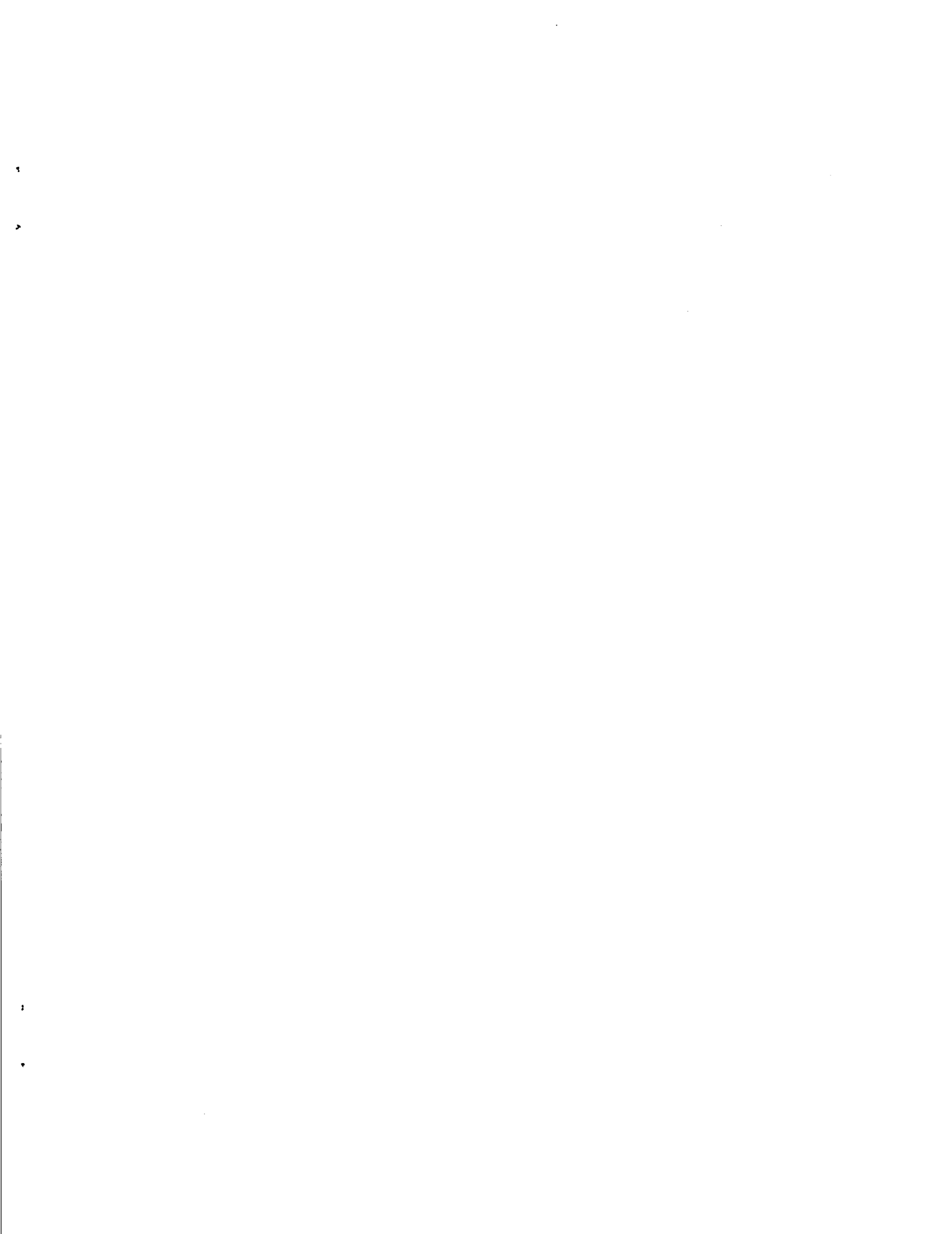


Figure 6. - Continued.

Figure 6. - Concluded.



1. Report No. NASA TM-83593	2. Government Accession No.	3. Recipient's Catalog No.	
4. Title and Subtitle Real-Time Simulation of an Automotive Gas Turbine using the Hybrid Computer		5. Report Date May 1984	
7. Author(s) William Costakis and Walter C. Merrill		6. Performing Organization Code 505-34-02	
9. Performing Organization Name and Address National Aeronautics and Space Administration Lewis Research Center Cleveland, Ohio 44135		8. Performing Organization Report No. E-1994	
12. Sponsoring Agency Name and Address U.S. Department of Energy Office of Vehicle and Engine R&D Washington, D.C. 20545		10. Work Unit No.	
		11. Contract or Grant No.	
		13. Type of Report and Period Covered Technical Memorandum	
		14. Sponsoring Agency Code Report No. DOE/NASA/51040-52	
15. Supplementary Notes Final report. Prepared under Interagency Agreement DE-AI01-77CS51040.			
16. Abstract A hybrid computer simulation of an Advanced Automotive Gas Turbine Powertrain System is reported. The system consists of a gas turbine engine, an automotive drivetrain with four-speed automatic transmission, and a control system. Generally, dynamic performance is simulated on the analog portion of the hybrid computer while most of the steady-state performance characteristics are calculated to run faster than real-time and makes this simulation a useful tool for a variety of analytical studies.			
17. Key Words (Suggested by Author(s)) Automotive gas turbine Hybrid computer Simulation		18. Distribution Statement Unclassified - unlimited STAR Category 85 DOE Category UC-96	
19. Security Classif. (of this report) Unclassified	20. Security Classif. (of this page) Unclassified	21. No. of pages 13	22. Price* A02

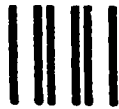


National Aeronautics and
Space Administration

Washington, D.C.
20546

Official Business
Penalty for Private Use, \$300

SPECIAL FOURTH CLASS MAIL
BOOK



Postage and Fees Paid
National Aeronautics and
Space Administration
NASA-451

NASA

POSTMASTER: If Undeliverable (Section 15K
Postal Manual) Do Not Return
